

# Anderson transition in the three dimensional symplectic universality class

Yoichi Asada<sup>1</sup>, Keith Slevin<sup>1</sup>, and Tomi Ohtsuki<sup>2</sup>

<sup>1</sup>*Department of Physics, Graduate School of Science, Osaka University, 1-1 Machikaneyama, Toyonaka, Osaka 560-0043, Japan*

<sup>2</sup>*Department of Physics, Sophia University, Kioi-cho 7-1, Chiyoda-ku, Tokyo 102-8554, Japan*

We study the Anderson transition in the SU(2) model and the Ando model. We report a new precise estimate of the critical exponent for the symplectic universality class of the Anderson transition. We also report numerical estimation of the  $\beta$  function.

KEYWORDS: Anderson transition, symplectic class, spin-orbit coupling, critical exponent, beta function

## 1. Introduction

The Anderson transition is a continuous zero temperature quantum phase transition. Just like continuous thermal phase transitions, such as the magnetic phase transition in spin systems, the critical phenomena of the Anderson transition are described by the single parameter scaling hypothesis.<sup>1</sup> It is thought that there are three universality classes: orthogonal, unitary, and symplectic. In the absence of an applied magnetic field or other effect that breaks time reversal symmetry, disordered electron systems with spin-orbit coupling belong to the symplectic universality class. Such systems are the subject of this proceeding.

One of the important quantitative characteristics of the Anderson transition is the critical exponent  $\nu$  that describes the divergence of the localization length  $\xi$

$$\xi \propto |x - x_c|^{-\nu}. \quad (1)$$

Here  $x$  is a parameter such as strength of disorder, Fermi energy, and  $x_c$  is its critical value. For the orthogonal and unitary universality classes,  $\nu$  has been determined with high precision:  $\nu = 1.57 \pm 0.02$  for the orthogonal class<sup>2</sup> and  $\nu = 1.43 \pm 0.04$  for the unitary class<sup>3</sup> in three dimension (3D) with 95% confidence intervals. By comparing the numerical estimates of the critical exponent in different models, the universality of these values has also been tested.<sup>2,3</sup>

The value of the critical exponent is expected to be helpful in identifying the mechanism that drives the metal-insulator transition observed in doped semiconductors and amorphous materials. The theoretically estimated value  $\nu$  can be compared with the experimentally measured conductivity exponent  $\mu$

$$\sigma(T=0) \propto (x - x_c)^\mu, \quad (2)$$

through Wegner's relation<sup>4</sup>  $\mu = (d-2)\nu$ ,  $d$  being the dimensionality of the system; this predicts  $\mu = \nu$  in 3D. Here  $\sigma(T=0)$  is the conductivity at zero temperature.

In early work, the exponent  $\mu$  was estimated by extrapolating the conductivity to zero temperature. More recent work avoids this unstable extrapolation by using finite temperature scaling.<sup>5</sup> This permits not only an estimation of the critical parameters but also a check of the validity of the single parameter scaling theory.

Various estimates of the exponent  $\mu$  have been ob-

tained experimentally (see Ref. 6 and references therein). Some claim  $\mu \approx 0.5$ , which seems to violate Chayes *et al.*'s inequality<sup>7,8</sup>  $\nu \geq 2/3$ . (Note that according to Wegner's relation  $\mu = \nu$ .) Stupp *et al.*<sup>9,10</sup> and Itoh *et al.*<sup>6</sup> pointed out that  $\mu \approx 0.5$  is obtained when data that may not be sufficiently close to the critical point are analyzed. When such data are excluded they found that  $\mu \approx 1$  is always valid.

The value  $\mu \approx 1$  is at variance with the theoretical values for the 3D orthogonal and unitary classes. To help clarify the origin of the discrepancy, a precise theoretical estimate for the 3D symplectic class is desirable. Furthermore, research in spintronics has sparked renewed interest in the effects of the spin-orbit interaction on quantum transport.<sup>11,12</sup>

In this proceeding, we report precise analyses of the critical phenomena at the Anderson transition in the SU(2) model<sup>13,14</sup> and the three dimensional generalization of the Ando model,<sup>15,16</sup> both of which have spin-orbit coupling and have symplectic symmetry. We also extend our finite size scaling analysis beyond the critical region and present a numerical estimate of the  $\beta$  function.

## 2. Model and method

The Hamiltonian used in this study describes non-interacting electrons on a square lattice with nearest neighbor hopping

$$H = \sum_{i,\sigma} \epsilon_i c_{i\sigma}^\dagger c_{i\sigma} - \sum_{\langle i,j \rangle, \sigma, \sigma'} R(i,j)_{\sigma\sigma'} c_{i\sigma}^\dagger c_{j\sigma'}. \quad (3)$$

We distribute the random potential  $\epsilon_i$  with box distribution in the range  $[-W/2, W/2]$ . Spin-orbit coupling is included in the  $2 \times 2$  matrix  $R(i,j)$ .

In the Ando model, the hopping matrix depends only on the direction

$$R(i, i + \mathbf{e}_n) = e^{i\theta\sigma_n} \quad (n = x, y, z), \quad (4)$$

where  $\mathbf{e}_n$  is the unit vector in the  $n$  direction and  $\sigma_n$  is the Pauli spin matrix. The parameter  $\theta$ , which is set to be  $\theta = \pi/6$  in our simulation, represents the strength of spin-orbit coupling.

In the SU(2) model, the hopping matrix  $R(i,j)$  is distributed randomly and independently with uniform probability on the group SU(2) according to the group invari-

ant measure. We parametrize the matrix  $R(i, j)$  as

$$R(i, j) = \begin{pmatrix} e^{i\alpha_{ij}} \cos \beta_{ij} & e^{i\gamma_{ij}} \sin \beta_{ij} \\ -e^{-i\gamma_{ij}} \sin \beta_{ij} & e^{-i\alpha_{ij}} \cos \beta_{ij} \end{pmatrix}. \quad (5)$$

and distribute  $\alpha$  and  $\gamma$  with uniform probability in the range  $[0, 2\pi)$ , and  $\beta$  according to the probability density,  $P(\beta)d\beta = \sin(2\beta)d\beta$  in the range  $[0, \pi/2]$ .

We consider a quasi-1D bar of cross section  $L^2$ . Periodic boundary conditions are imposed in the transverse directions. We calculate the quasi-1D localization length  $\lambda$  with the transfer matrix method<sup>17,18</sup> and analyze the finite size scaling of the dimensionless parameter  $\Lambda = \lambda/L$ . In our simulation we fixed the Fermi energy  $E = 0$  and accumulated the data by varying disorder  $W$  and system size  $L$ .

The single parameter scaling hypothesis implies that  $\Lambda$  obeys

$$\ln \Lambda = F_{\pm} \left( \frac{L}{\xi} \right). \quad (6)$$

Here  $\xi$  is the correlation length in the metallic phase and the localization length in the localized phase. The subscript  $\pm$  distinguishes the scaling function in the metallic and localized phases. When we analyze the critical phenomena of the Anderson transition, it is more useful to use a different but equivalent form of the single parameter scaling law

$$\ln \Lambda = F_0(L^{1/\nu}\psi). \quad (7)$$

Here  $\psi$  is a smooth function of disorder  $W$  that crosses zero linearly at the critical point  $W = W_c$ .

Single parameter scaling of  $\Lambda$  can be described by the  $\beta$  function<sup>14,18</sup>

$$\beta(\ln \Lambda) = \frac{d \ln \Lambda}{d \ln L}. \quad (8)$$

We estimate the  $\beta$  function from the finite size scaling analyses of numerical data. The  $\beta$  function in the critical region is calculated from  $F_0$  and the critical exponent  $\nu$ , and outside the critical region from  $F_{\pm}$ .

### 3. Critical phenomena of the Anderson transition

We calculate  $\Lambda$  for sizes  $L = 4, 5, 6, 8, 10, 12, 14$  with an accuracy of 0.1%. The numerical data and the associated fits are shown in Figs. 1 and 2. In the absence of any irrelevant corrections to single parameter scaling Eq. (7), plotting  $\Lambda$  vs  $W$  should show the critical disorder as the common crossing point of the data. However, the curves for different sizes in Figs. 1 and 2 do not cross at a common point, indicating the existence of irrelevant corrections to single parameter scaling.<sup>2</sup> Such corrections to perfect single parameter scaling are usually present in a simulation of a finite system.

To analyse data over the full range of system sizes  $L = [4, 14]$ , we must take account of corrections to single parameter scaling due to an irrelevant variable,<sup>2</sup>

$$\ln \Lambda = F_0(\psi L^{1/\nu}) + \phi L^y F_1(\psi L^{1/\nu}). \quad (9)$$

where  $y$  is an irrelevant exponent and  $\phi L^y$  is the corresponding irrelevant scaling variable. For the purpose of

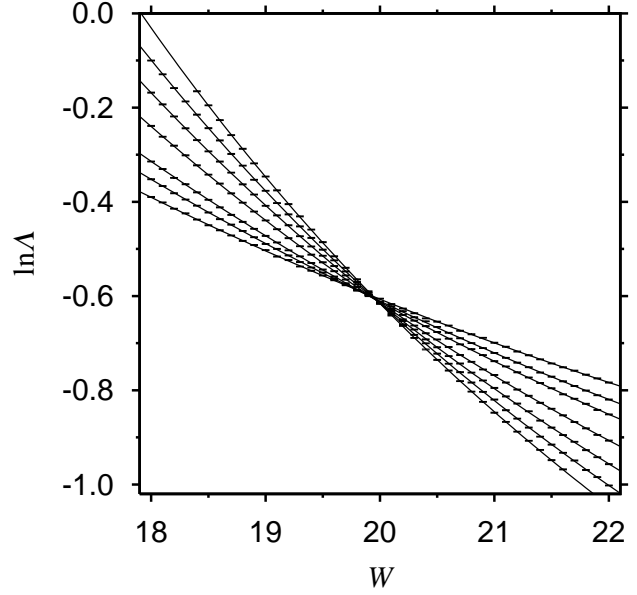


Fig. 1.  $\ln \Lambda$  as a function of disorder  $W$  for the SU(2) model. The lines are the fit to the function  $(n_R, n_I, m_R, m_I) = (3, 1, 2, 0)$ . Although it may be difficult to confirm the existence of corrections to single parameter scaling in this figure, finite size scaling fit shows that such corrections do exist.

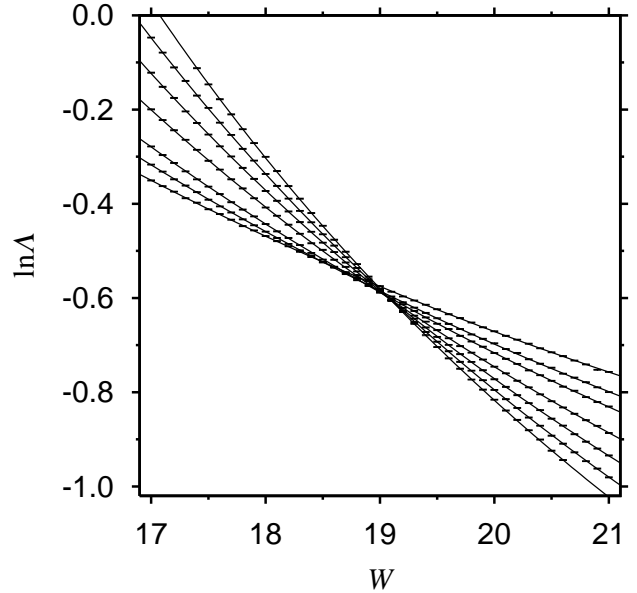


Fig. 2.  $\ln \Lambda$  as a function of disorder  $W$  for the Ando model. The lines are the fit to the function  $(n_R, n_I, m_R, m_I) = (3, 1, 2, 0)$ . There are relatively larger irrelevant corrections to single parameter scaling.

fitting, we approximate  $F_0$  and  $F_1$  by their finite order expansions

$$F_0(x) = \ln \Lambda_c + x + a_2 x^2 + \cdots + a_{n_R} x^{n_R} \quad (10)$$

$$F_1(x) = 1 + b_1 x + \cdots + b_{n_I} x^{n_I}. \quad (11)$$

We also expand  $\psi$  and  $\phi$  in terms of the dimensionless

Table I. The details of various analyses where irrelevant corrections to single parameter scaling are considered, and the best fit estimates of the critical parameters.  $N_d$  is the number of data used in each analysis,  $N_p$  is the number of parameters,  $Q$  is the goodness of fit probability. The precision is expressed as 95% confidence intervals.

Model	$L$	$N_d$	$n_R$	$n_I$	$m_R$	$m_I$	$N_p$	$Q$	$W_c$	$\ln \Lambda_c$	$\nu$	$y$
SU(2)	[4,14]	279	3	1	2	0	10	0.92	$20.001 \pm .017$	$-0.616 \pm .005$	$1.375 \pm .016$	$-2.5 \pm .8$
Ando	[4,14]	279	3	1	2	0	10	0.9	$19.099 \pm .009$	$-0.605 \pm .002$	$1.360 \pm .006$	$-3.8 \pm .4$

Table II. The details of analyses where corrections to scaling are neglected. The precision is again expressed as 95% confidence intervals.

Model	$L$	$N_d$	$n_R$	$m_R$	$N_p$	$Q$	$W_c$	$\ln \Lambda_c$	$\nu$
SU(2)	[8,14]	156	3	2	7	0.7	$19.984 \pm .008$	$-0.612 \pm .002$	$1.367 \pm .007$
Ando	[10,14]	115	3	2	7	0.6	$19.092 \pm .013$	$-0.603 \pm .003$	$1.361 \pm .011$

disorder  $w = (W_c - W)/W_c$ ,

$$\psi = \psi_1 w + \psi_2 w^2 + \cdots + \psi_{m_R} w^{m_R} \quad (12)$$

$$\phi = \phi_0 + \phi_1 w + \cdots + \phi_{m_I} w^{m_I}. \quad (13)$$

The details and results of the analyses are presented in Table I.

By discarding data for smaller systems, an analysis of the data that neglects irrelevant corrections becomes possible. A reasonable fit is obtained in the SU(2) model for  $L \geq 8$  and in the Ando model for  $L \geq 10$  (Table II). The estimated critical parameters in Table II are in reasonable agreement with those in Table I.

The most important point to be drawn from Table I and Table II is that the estimates of the exponent  $\nu$  for the SU(2) model and the Ando model are in almost perfect agreement. As for the irrelevant exponent  $y$ , our estimates are much less precise and we can not clarify whether the values of  $y$  for these two models are the same or not.

Figures 1 and 2 show that the movement of the crossing points in the SU(2) model is smaller than that in the Ando model, indicating that the magnitude of irrelevant corrections in the SU(2) model is smaller. At the same time, we can expect that the spin relaxation length is shorter in the SU(2) model because of the random spin-orbit coupling. This suggests that the leading irrelevant corrections observed for small  $L$  in the Ando model might be from its relatively larger spin relaxation length.

#### 4. Estimation of the $\beta$ function

We estimate the  $\beta$  function Eq. (8) by accumulating more numerical data in the metallic and localized regions of the SU(2) model at  $E = 0$ . The ranges of disorder and system size are  $W = [4, 19]$  and  $L = [8, 14]$  for the metallic phase,  $W = [21, 30]$  and  $L = [8, 16]$  for the localized phase. The precision of the data for  $\Lambda$  is 0.3% or 0.6%. The data covers the strongly localized to the strongly metallic limits.

We perform five scaling analyses for five regions: strongly localized, localized, critical, metallic, and strongly metallic. From these analyses we estimate the  $\beta$  function. The methods of analyses are almost the same as those used in 2D,<sup>14</sup> so we do not describe them in detail here. We mention only one difference in the strongly metallic region. As discussed in Ref. 18, the asymptotic

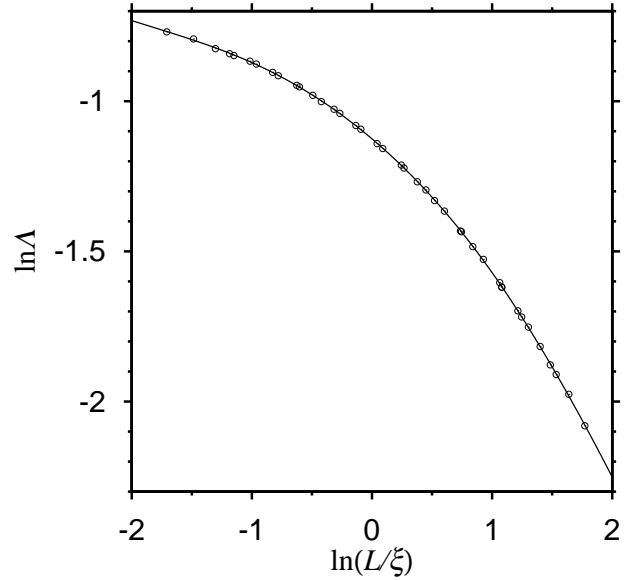


Fig. 3. Single parameter scaling in the localized region is demonstrated.

value of  $\beta(\ln \Lambda)$  may depend on the dimensionality  $d$

$$\beta(\ln \Lambda) \rightarrow d - 2 \quad (\ln \Lambda \rightarrow \infty). \quad (14)$$

We analyze the data in the strongly metallic region supposing that the asymptotic value is one in 3D. For large but finite  $\Lambda$  we speculate that derivations from the asymptotic value can be described by an expansion in powers of  $\Lambda^{-1}$ . Stopping at the first order we have

$$\beta(\ln \Lambda) = 1 + \frac{b}{\Lambda} \quad (\Lambda \gg 1). \quad (15)$$

This corresponds to a linear increase of  $\Lambda$  with  $L$

$$\Lambda = a \frac{L}{\xi} - b \quad (\Lambda \gg 1). \quad (16)$$

Numerical data for large  $\Lambda$  are well fitted by this form.

In Figs. 3 and 4 we demonstrate the single parameter scaling in the localized and metallic region. We can see from these figures that the data for different values of disorder  $W$  and system size  $L$  fall on a common scaling curve when expressed as a function of  $L/\xi$ .

The resulting  $\beta$  function is displayed in Fig. 5 as well as

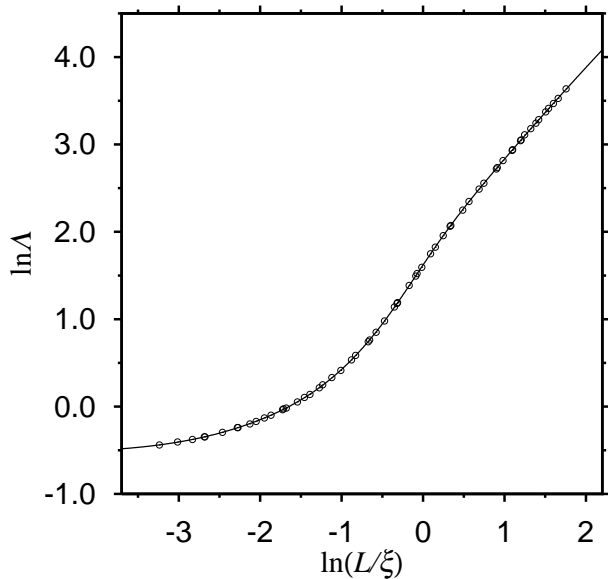


Fig. 4. Single parameter scaling in the metallic region is demonstrated.

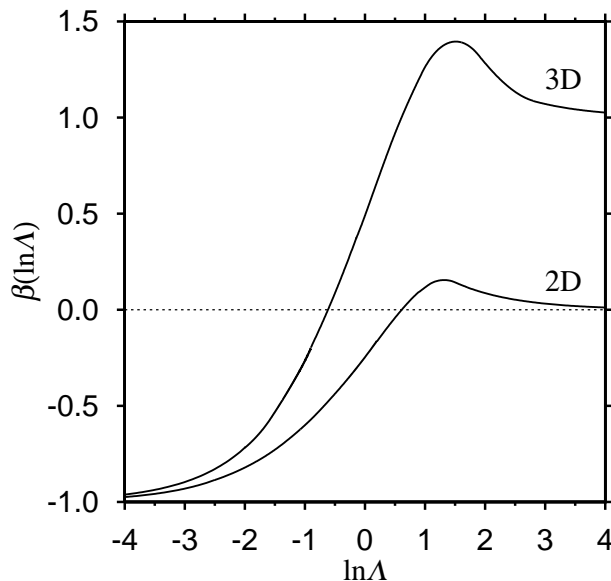


Fig. 5. The  $\beta$  functions for  $\Lambda$ . The  $\beta$  function in 2D is from Ref. 14.

the  $\beta$  function in 2D, which is reported in Ref. 14. The  $\beta$  functions show non-monotonic behavior. The maximum values are  $\beta_{max} \approx 1.40$  in 3D and  $\beta_{max} \approx 0.15$  in 2D.

## 5. Summary and Discussion

In summary, we analyzed the scaling of the parameter  $\Lambda$  in 3D. The critical phenomena of the Anderson

transition in the SU(2) model and the Ando model are analyzed and the critical exponent is estimated with high precision. All the estimates of the critical exponent are in the range  $\nu = [1.35, 1.39]$ . Our estimate is consistent with the previous estimates  $\nu = 1.3 \pm 0.2$ <sup>19</sup> and  $\nu = 1.36 \pm 0.10$ <sup>20</sup> for the symplectic class. We also estimated the  $\beta$  function over the full range from the localized to the metallic limits.

Our precise estimate clearly distinguishes the value of the critical exponent  $\nu$  in the symplectic class from that for the orthogonal class  $\nu = 1.58 \pm 0.02$ .<sup>2</sup> On the other hand, comparing with the available estimate<sup>3</sup>  $\nu = 1.43 \pm 0.04$  for the unitary class, the precision is not yet sufficient to allow the same statement to be made, although the theoretical expectation is that the values for the unitary and symplectic classes should be different, as was clearly demonstrated in 2D.<sup>13, 14, 21</sup>

The values of the critical exponent for three universality classes of the Anderson transition are inconsistent with the exponent  $\mu \approx 1$  measured in experiment. This may indicate that the observed transition is not a pure Anderson transition and that electron-electron interaction effects may have to be taken into account to properly account for the critical phenomena.<sup>5</sup>

- 1) E. Abrahams, P. W. Anderson, D. C. Licciardello, and T. V. Ramakrishnan: Phys. Rev. Lett. **42** (1979) 673.
- 2) K. Slevin and T. Ohtsuki: Phys. Rev. Lett. **82** (1999) 382.
- 3) K. Slevin and T. Ohtsuki: Phys. Rev. Lett. **78** (1997) 4083.
- 4) F. Wegner: Z. Phys. B **25** (1976) 327.
- 5) D. Belitz and T. R. Kirkpatrick: Rev. Mod. Phys. **66** (1994) 261.
- 6) K. M. Itoh, M. Watanabe, Y. Ootuka, E. E. Haller, and T. Ohtsuki: J. Phys. Soc. Jpn. **73** (2004) 173.
- 7) J. T. Chayes, L. Chayes, D. S. Fisher and T. Spencer: Phys. Rev. Lett. **57** (1986) 2999.
- 8) B. Kramer: Phys. Rev. B **47** (1993) 9888.
- 9) H. Stupp, M. Hornung, M. Lakner, O. Madel and H. v. Löhneysen: Phys. Rev. Lett. **71** (1993) 2634.
- 10) H. Stupp, M. Hornung, M. Lakner, O. Madel and H. v. Löhneysen: Phys. Rev. Lett. **72** (1994) 2122.
- 11) I. Žutić, J. Fabian and S. Das Sarma: Rev. Mod. Phys. **76** (2004) 323.
- 12) S. Murakami, N. Nagaosa and S.-C. Zhang: Science **301** (2003) 1348.
- 13) Y. Asada, K. Slevin, and T. Ohtsuki: Phys. Rev. Lett. **89** (2002) 256601.
- 14) Y. Asada, K. Slevin, and T. Ohtsuki: Phys. Rev. B **70** (2004) 035115.
- 15) T. Ando: Phys. Rev. B **40** (1989) 5325.
- 16) K. Slevin, J.-L. Pichard, and P. A. Mello: J. Phys. I (France) **6** (1996) 529.
- 17) J.-L. Pichard and G. Sarma: J. Phys. C **14** (1981) L127.
- 18) A. MacKinnon and B. Kramer: Z. Phys. B **53** (1983) 1.
- 19) T. Kawarabayashi, T. Ohtsuki, K. Slevin, Y. Ono: Phys. Rev. Lett. **77** (1996) 3593.
- 20) E. Hofstetter: Phys. Rev. B **57** (1998) 12763.
- 21) B. Huckestein: Rev. Mod. Phys. **67** (1995) 357.